

Review

**A mathematical analysis of the characteristics of the system
connecting the cerebellar ventral paraflocculus and
extraoculomotor nucleus of alert monkeys during upward ocular
following responses**

Kenji Yamamoto ^{a,b,*}, Yasushi Kobayashi ^c, Aya Takemura ^{b,d}, Kenji Kawano ^{b,d},
Mitsuo Kawato ^e

^a *Japan Science and Technology Corporation, Domestic Research Fellow, Tsukuba, Ibaraki 305-8568, Japan*

^b *Neuroscience Section, Electrotechnical Laboratory, 1-1-4, Umezono, Tsukuba, Ibaraki 305-8568, Japan*

^c *National Institute for Physiological Sciences, Aichi 444-8585, Japan*

^d *CREST, Japan Science and Technology Corporation, Tsukuba, Ibaraki 305-8568, Japan*

^e *ATR Human Information Processing Research Laboratories, Kyoto 619-0288, Japan*

Received 18 May 2000; accepted 7 September 2000

Abstract

Movements of the visual scene evoke short-latency ocular-following-responses (OFR). Many studies suggest that a neural pathway containing the cerebellar-ventral-paraflocculus (VPFL) mediates OFR. The relationship between eye movement and simple-spike firing in the VPFL during OFR has been studied in detail using an inverse dynamics approach. The relationship between eye movement and cell firing in the extraoculomotor nucleus (MN) has already been reported. However, no studies have examined the information transformation that occurs between the VPFL and the MN during OFR. In this paper, using an inverse dynamics approach, we derive a transfer function that represents the characteristics of the structure connecting the VPFL and the MN during upward OFR. This structure appears to contain a kind of neural integrator, which constructs eye-velocity-and-position information from eye-acceleration-and-velocity information. We propose a diagram for the neural integration commonly at work during all types of upward eye movement. This is a closed-loop circuit containing a low-pass filter. The low-pass filter can construct eye-velocity-and-position information from an eye-acceleration-velocity-position command similar to the final motor command used commonly for all upward eye movements. Anatomical and electrophysiological data suggest that the vestibular nuclei-interstitial nucleus of Cajal-vestibular nuclei loop might perform such neural integration. © 2000 Elsevier Science Ireland Ltd and the Japan Neuroscience Society. All rights reserved.

Keywords: Ocular following; Ventral paraflocculus; Inverse dynamics analysis; Neural integrator; Monkey

1. Introduction

Behavioral studies in monkeys and humans have shown that sudden movements of the visual scene evoke short-latency ocular-following responses (OFR),

which are thought to be important for stabilizing the eyes on nearby stationary objects during movement of the observer (Miles et al., 1986; Gellman et al., 1990; for review see Kawano, 1999). The control system for OFR is assumed to be triggered by movement of the retinal image and to be a visual negative-feedback-system (Yamamoto et al., 1997a; Kawano, 1999). Evidence from single-unit recordings and focal chemical lesions suggests that OFR are mediated by a pathway that includes area MST of the cerebral cortex (Kawano et

* Corresponding author. Present address: Neuroscience Section, Electrotechnical laboratory, 1-1-4, Umezono, Tsukuba, Ibaraki 305-8568, Japan. Tel.: +81-298-615-848; fax: +81-298-615-849.

E-mail address: yamaken@etl.go.jp (K. Yamamoto).

al., 1994), the dorsolateral pontine nucleus (DLPN) (Kawano et al., 1992), and the ventral parafloccular lobes of the cerebellum (VPFL) (Miles et al., 1986; Shidara and Kawano, 1993). However, it is not clear what informational processing occurs between the VPFL and the extraoculomotor nucleus (MN) during OFR.

Using an inverse dynamics approach, Shidara et al. (1993) and Gomi et al. (1998) showed that the temporal modulation pattern of the simple-spike discharge of Purkinje cells in the VPFL during OFR can be reconstructed from simple-spike firing by combining the acceleration, velocity, and position of eye movements with a time delay. The time delay was near the latency of electrical-stimulation-evoked eye movements.

In the inverse dynamics analysis, the temporal firing patterns are fitted by kinetic information containing a motor apparatus. With best-fit parameter values, we can examine which portion of the final motor command is represented by the temporal pattern of the instantaneous firing frequency of neurons in a brain region under consideration (Gomi et al., 1998). If firing patterns can be well reconstructed by an inverse dynamics representation, we can then understand not only what information is encoded in that neural activity, but also which portion of the motor command is still lacking. This should allow us to suggest the downstream neural structures and parallel pathways necessary to construct the final motor command.

Using the inverse dynamics approach, this paper examines the characteristics of the system between the VPFL and the MN during upward OFR. First, from an inverse dynamics analysis of our physiologically recorded data, we derive a transfer function that represents the characteristics of the system. Then, we analyze what kinds of processing must occur in the system and propose block diagrams equivalent to the transfer function. Finally, we propose a plausible algorithm for the neural integration in the brain stem necessary to control upward OFR.

Preliminary reports of this study have appeared previously (Yamamoto et al., 1997b).

2. Method

Our analysis was based on recordings of eye movements and simple spike activity of Purkinje cells in the VPFL, as described in a previous paper (Kobayashi et al., 1998). The methods for preparing monkeys, presenting visual stimuli, and recording the simple spike and eye movements are described in Gomi et al. (1998) and Kobayashi et al. (1998). Briefly, data were collected from two Japanese monkeys (*Macaca fuscata*) that had been trained to fixate on a small spot. Under pentobarbital sodium anesthesia and aseptic conditions, a head

holder, a cylinder for microelectrode recording, and scleral search coils for measuring eye movements were implanted in the monkeys. The animals faced a tangent screen, upon which random dot patterns were back-projected and moved at a constant velocity (80° s^{-1} upward) to elicit ocular following. VPFL simple spike activity and eye movement were recorded simultaneously. In one monkey, the eye movements and simple spike firing of 11 cells were recorded during 5,719 trials. In the other monkey, the eye movements and simple spike firing of one Purkinje cell were recorded during 99 trials. The data for the 1 ms bin during the first 285 ms after the onset of visual stimuli motion were averaged over all cells and trials for each monkey.

To determine the accuracy of the models for the system between the VPFL and eye movement, we simulated eye movements from recorded simple spike firing frequency. The accuracy of the simulated eye movements (goodness-of-fit) was estimated with the following equation:

$$R^2 = 1 - \left\{ \frac{\sum (\hat{f}(t) - f(t))^2}{\sum (f(t) - \bar{f})^2} \right\}$$

$\hat{f}(t)$ represents the simulated eye movement, $f(t)$ represents the recorded eye movement of the monkey, and \bar{f} represents the average of $f(t)$. The accuracy of the simulated results increases as R approaches 1.

First, we analyzed the data for 5,719 trials in one monkey in detail. Then, we analyzed the data for 99 trials in the other monkey.

3. Results

3.1. Inverse dynamics representation of neural discharge

Shidara et al. (1993) and Gomi et al. (1998) successfully reconstructed the temporal firing frequency pattern of simple spikes by summing the acceleration, velocity, and position of eye movements using the following Eq. (1).

$$s(t) = M_{\text{ES}} \cdot \ddot{\theta}(t + \delta) + B_{\text{ES}} \cdot \dot{\theta}(t + \delta) + K_{\text{ES}} \cdot \theta(t + \delta) + C_{\text{ES}} \quad (1)$$

Where, $s(t)$, $\ddot{\theta}(t)$, $\dot{\theta}(t)$, $\theta(t)$, δ , and C_{ES} are the simple spike firing frequency at time t , the eye acceleration, velocity, and position at time t , the time lag between the firing frequency and the eye movement, and a bias term, respectively. The coefficients M_{ES} , B_{ES} , K_{ES} , and C_{ES} , and the time lag δ are parameters. Eq. (1) means that the system between the VPFL and eye movements works as a second-order low pass filter, as a Laplace transfer function (Fig. 1A).

Based on statistical analyses, Gomi et al. (1998) concluded that the VPFL simple spike firing frequency

for downward OFR contains positional information on eye movements, while Yamamoto et al. (1997a) concluded that the simple spike firing frequency for upward OFR does not contain positional information on eye movements. They successfully reconstructed the temporal pattern of simple spike firing during upward OFR by combining the eye acceleration and velocity data, suggesting that the simple spike firing during upward OFR contains an eye acceleration-velocity command. Based on this report, the eye-position coefficient K_{ES} in Eq. (1) was set at zero in the present study of upward OFR.

C_{ES} in Eq. (1) was approximated as the mean simple spike firing rate between 0–30 ms after the onset of visual stimulus motion. Values of the parameters M_{ES} , B_{ES} , and δ were estimated to minimize the squared error between the observed and reconstructed firing frequencies.

In an inverse dynamics representation, the final motor command $mc(t)$ as the firing frequency of MN neurons is represented by the following Eq. (2);

$$mc(t) = \tilde{M}_{EM} \ddot{\theta}(t + \Delta) + \tilde{B}_{EM} \dot{\theta}(t + \Delta) + \tilde{K}_{EM} \theta(t + \Delta) + \tilde{C}_{EM} \quad (2)$$

where, \tilde{M}_{EM} , \tilde{B}_{EM} , \tilde{K}_{EM} , \tilde{C}_{EM} , and Δ are coefficients for eye acceleration, velocity, position, the bias term, and the time lag, respectively. Eq. (2) means the system between the MN and eye movement works as a second-order low pass filter, as a Laplace transfer function (Fig. 1B).

Keller (1973) reported the time constants of the low pass filter for the system between the firings of medial and lateral recti motoneurons and horizontal eye movement, while there are no reports on the detailed characteristics of the firing of motoneurons for vertical eye movements. In this paper, we use coefficients in Eq. (2) based on the data and time constants reported by Keller (1973) for the upward OFR on the assumption that the coefficients are not very different between horizontal and vertical motoneurons. Thus, \tilde{M}_{EM} , \tilde{B}_{EM} , and \tilde{K}_{EM} were estimated as 0.012, 0.808, and 4.14, respectively.¹

The reported time lag from the electrical stimulation of the cerebellar flocculus to inhibition of the flocculus-target-neurons in the VN was 1.0 ± 0.57 ms, and the time lag from electrical stimulation of the

oculomotor nucleus to antidromic responses of flocculus-target-neurons in the VN was 0.58 ± 0.07 ms (Zhang et al., 1995). The time lag was estimated at 7.50 ± 4.24 ms from Eq. (1) (Gomi et al., 1998), indicating that the time lag from simple spike firing to eye movement (δ) is almost the same as the time lag from firing in the MN to eye movement (Δ). Therefore, in this study, we assume that $\delta = \Delta$, to simplify the analysis. The bias terms, C_{EM} and \tilde{C}_{ES} , correspond to the spontaneous activity of the simple spike and the MN. In this study, we assume that $\tilde{C}_{EM} = C_{ES}$, to simplify the analysis.

3.2. Characteristics of the system connecting the VPFL and the MN

Using the data for the 5,719 trials in 11 cells of one monkey with upward stimuli at 80 deg s^{-1} , the parameters M_{ES} and B_{ES} in Eq. (1) (or Fig. 1A) were estimated to be 0.0245 and 0.818, respectively.

A transfer function with the characteristics of the system between the VPFL and the MN was derived from the transfer functions in Fig. 1A and Fig. 1B and estimated as that in the left box in Fig. 1C. Inputting a recorded temporal pattern of the simple spike firing frequency of the monkey (black line in Fig. 1D-a) into the left box in Fig. 1C generated a reconstructed temporal pattern of the firing frequency in the MN (red line in Fig. 1D-a). Inputting this reconstructed temporal pattern into the middle box in Fig. 1C, which is the same as the left box in Fig. 1B, generated a reconstructed temporal pattern of eye position (red line in Fig. 1D-c). The reconstructed eye positions were almost the same as the recorded eye positions of the monkey (black line in Fig. 1D-c). The goodness-of-fit between the reconstructed eye positions and the recorded eye positions in Fig. 1D-c was 0.999.

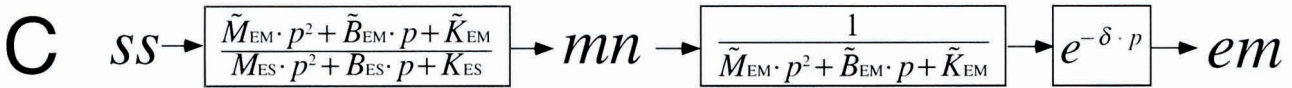
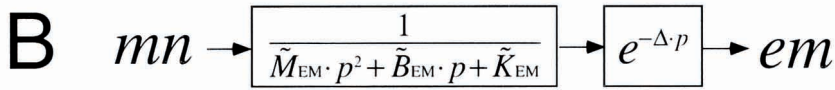
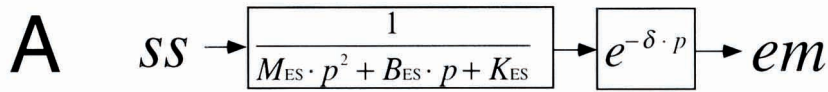
We compared the parameters in Eq. (1) and Eq. (2) to understand what kind of information transformation was performed between the VPFL and the MN. If the ratios of the parameters in Eq. (1) and Eq. (2), i.e. M_{ES}/\tilde{M}_{EM} , B_{ES}/\tilde{B}_{EM} , and K_{ES}/\tilde{K}_{EM} , are equal, simple spike firing is assumed to be enough to construct the final motor command. If the ratios differ, the simple spike firing is not enough to construct the final motor command. The respective ratios were 2.04, 1.01, and 0, indicating that simple spike firing is not sufficient for the final motor command and some ‘missing’ motor command is required in addition to simple spike firing to construct the final motor command.

The larger ratio for the acceleration coefficient (2.04) than those for the velocity and position coef

¹ Keller (1973) reported that the average time constants using the second-order equation for the firing of 15 units in the extraoculomotor nucleus were 16.2 ms for the smaller time constant and 179 ms for the larger time constant. He also reported that the coefficient for the eye acceleration term in the second-order equation was 0.012 for a specific example unit. Using these time constants and coefficient, we calculated the coefficients \tilde{M}_{EM} , \tilde{B}_{EM} , and \tilde{K}_{EM} in Eq. 2 as 0.012, 0.808, and 4.14, respectively.

cients (1.01 and 0, respectively) means that simple spikes make a larger contribution to the final acceleration command than to final velocity and position

commands. Accordingly, in this paper, we assume that the final acceleration command in the final motor command comes from simple spike firing.



D

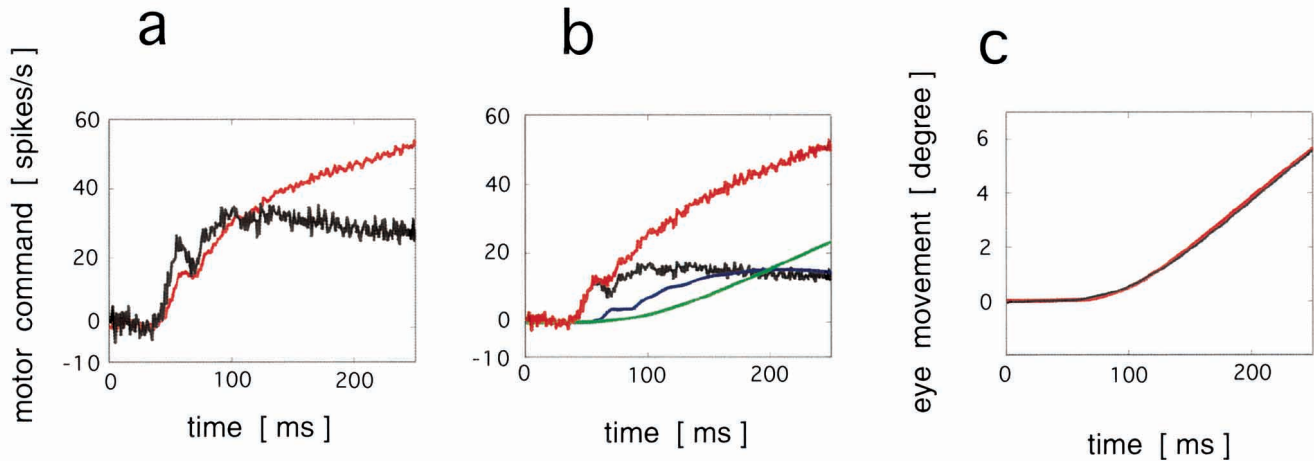


Fig. 1.

If we assume that all the final acceleration command for upward OFR is served by simple spikes and that the system between the VPFL and the MN serves to amplify the acceleration command, the simple spike firing frequency is transported into the brain stem after multiplying it by \tilde{M}_{ES}/M_{ES} . Accordingly, we can calculate the ‘missing’ motor command by subtracting \tilde{M}_{ES}/M_{ES} times Eq. (1) from Eq. (2);

$$\begin{aligned} & \text{‘missing’ motor command}(t) \\ &= mc(t) - (\tilde{M}_{EM}/M_{ES})s(t) \\ &= \{\tilde{B}_{EM} - (\tilde{M}_{EM}/M_{ES})B_{ES}\}\dot{\theta}(t + \delta) \\ & \quad + \{\tilde{K}_{EM} - (\tilde{M}_{EM}/M_{ES})K_{ES}\}\theta(t + \delta) \\ &= 0.407\dot{\theta}(t + \delta) + 4.14\theta(t + \delta) \end{aligned} \quad (3)$$

The ‘missing’ motor command calculated was $0.407\dot{\theta} + 4.14\theta$. This indicates that eye velocity and position commands must be added to simple spike firing between the VPFL and the MN. The ‘missing’ command to construct the final motor command is $0.407/0.808 = 0.5$ times the final eye velocity command, and $4.14/4.14 = 1$ times the final eye position command. This ‘missing’ eye-velocity-position command must be added to the eye-acceleration-velocity command of simple spike firing to construct the final eye-acceleration-velocity-position command. Fig. 1D-b shows the temporal firing pattern of the MN (red line) reconstructed by summing 0.012/0.0245 times the simple spike firing (black line) and 0.407 times eye velocity (blue line) and 4.14 times position (green line). The reconstructed temporal firing pattern (red line in Fig. 1D-b) is similar to the previously described reconstructed pattern in Fig. 1D-a (red line). The similarity between the reconstructed patterns from Eq. (2) (Fig. 1D-a, red line) and Eq. (3) (Fig. 1D-b, red line) means that the inverse dynamics representation of simple spike firing in Eq. (1) is very accurate.

Using the data for the 99 trials in the second monkey, during upward OFR with 80° s^{-1} stimuli, the coefficients for $s(t)$, $\dot{\theta}$, and θ in Eq. (3) were estimated to be 0.181, 0.389, and 4.14, respectively. This means that $0.389\dot{\theta} + 4.14\theta$ was the ‘missing’ motor command,

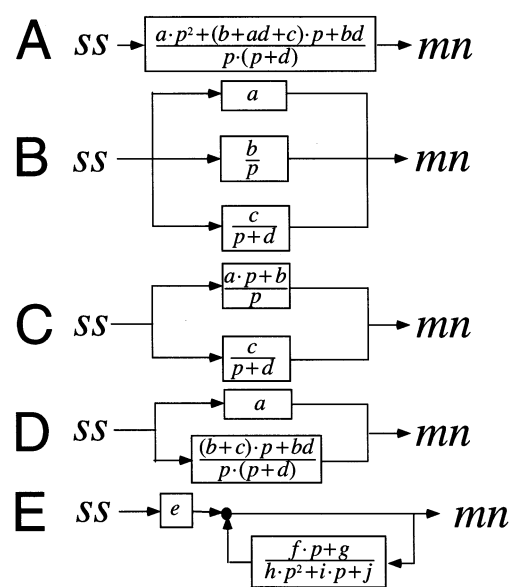


Fig. 2. Diagrams of models equivalent to the box on the left in Fig. 1C. The model shown in Fig. 2A is a cascade system; the models shown in Fig. 2B, Fig. 2C, and Fig. 2D are parallel systems, and the model shown in Fig. 2E is a system containing a closed feedback loop. p denotes a Laplace transformation operator. a , b , c , and d are 0.490, 5.06, 11.6, and 33.4, respectively. e , f , and g are 0.490, 0.407, and 4.14, respectively. h , i , and j are the same as \tilde{M}_{EM} , \tilde{B}_{EM} , and \tilde{K}_{EM} in Fig. 1C, respectively.

and it was very similar to the ‘missing’ motor command of the first monkey ($0.407\dot{\theta} + 4.14\theta$).

4. Discussion

4.1. An algorithm for creating a slow motor command during all types of upward eye movements

The characteristics of the system between the VPFL and the MN were estimated by the transfer functions in the block diagram on the left in Fig. 1C. Yamamoto et al. (1997a) concluded from a statistical analysis that the simple spike firing frequency for upward OFR does not contain the eye-position command. This means that we

Fig. 1. (A) Laplace transformation representation diagram showing the characteristics of the system between the VPFL and eye movement during upward OFR with upward stimuli at 80° s^{-1} . The transfer function in the left box shows the characteristics of the system between simple spikes (ss) of Purkinje cells in the VPFL and the eye movement position (em). The right box shows the transfer function for time-delay δ . p denotes a Laplace transformation operator. M_{ES} , B_{ES} , and K_{ES} , which are estimated by Eq. (1) and recorded simple spike firing and eye movements, are 0.012, 0.808, and 4.14, respectively. δ is 0.011 s. (B) Laplace transformation representation diagram showing the characteristics of the system between the firing of extraocular motor neurons (mn) and em during upward OFR with upward stimuli at 80° s^{-1} . The right box shows the transfer function for time-delay Δ . \tilde{M}_{EM} , \tilde{B}_{EM} , and \tilde{K}_{EM} , which are calculated from the data in Keller (1973), are 0.0245, 0.818, and 0, respectively. In this study, Δ is assumed to be the same as δ . (C) Laplace transformation representation diagram showing the characteristics of the system between ss and em . The box on the left shows the characteristics of the system between ss and mn . (D) a . The mean temporal firing frequency of the simple spikes (ss) of 11 Purkinje cells in the VPFL of one monkey for 5,719 trials (black line) and the temporal firing frequency of extraocular motor neurons (mn) simulated by the box on the left in (C) (red line). The line for ss shows firing below the spontaneous firing frequency. The line for mn shows increased firing over the bias term. b . Eq. (3) means that the sum of 0.012/0.0245 times ss (black line), 0.407 times eye velocity (blue line), and 4.14 times eye position (green line) corresponds to the temporal pattern of the firing frequency of mn (red line). c . The temporal pattern of the actual eye position of the monkey (black line) and that simulated by the system in Fig. 1C (red line).

can approximate K_{ES} in Eq. (1) as zero for upward OFR. In addition, it means zero can be used for K_{ES} in the box on the left in Fig. 1C for upward OFR. When $K_{ES} = 0$, the box on the left of Fig. 1C can be represented by several equivalent models, like those shown in Fig. 2. The model shown in Fig. 2A is a cascade system; the models shown in Fig. 2B, Fig. 2C, and Fig. 2D are parallel systems, and the model shown in Fig. 2E is a system containing a closed feedback loop. The systems in Fig. 2A, Fig. 2B, Fig. 2C, and Fig. 2D contain an integration element ($1/p$; p denotes a Laplace transformation operator), while the system in Fig. 2E contains a low-pass filter. The time constants of the second order low-pass filter in Fig. 2E are 16.2 and 179 ms (Keller, 1973). These values are much shorter than the time constant of leak of the neural integrator (about 25 s (Becker and Klein, 1973)) hypothesized to exist in the brain stem (Robinson, 1975).

To construct the final eye acceleration-velocity-position command from the eye acceleration-velocity command of simple spikes, some group of neurons in the brain stem must construct the ‘missing’ velocity-position command calculated by Eq. (3). Recordings of neural firing in the brain stem during VOR and saccades revealed that MN neurons produce mainly eye velocity and position commands, while other supranuclear sub-systems produce only eye velocity commands (for a review, see Robinson, 1975). Robinson (1975) suggested that an integrator in the brain stem performs the velocity-to-position transformation. During not only VOR and saccades but also OFR, the same neural system may construct the ‘missing’ eye velocity-position command from the eye acceleration-velocity command of the VPFL output.

To create the eye velocity-position command during not only OFR but also VOR and saccades, it is more efficient for the brain stem to have a common neural group that creates the velocity-position command during all types of eye movement than to have independent neuron groups that create the velocity-position command for each type of eye movement. If there is a common group of neurons for creating the slow motor command during all kinds of upward eye movement, it should receive commands for all types of each eye movement.

One possible neural structure that obviously receives commands during all types of upward eye movement is MN, because it is known that the motor commands for various kinds of eye movement converge at MN to move the eyes (for a review, see Robinson (1975)). Here, we assume that the common neural group receives the final motor command, which is the firing of MN, to construct the eye velocity-position command during all types of eye movement. The constructed eye velocity-position command is added to the eye acceleration-velocity command of simple spike firing to create the final motor command. Since the final motor command is fed into the common neural group, the system contains a closed-loop feedback

circuit. As we mentioned previously, the model shown in Fig. 2E contains such a closed-loop circuit. The low-pass filter in the closed-loop circuit of the model (Fig. 2E) is supposed to construct the eye-velocity-position command from the final motor command, i.e. the eye acceleration-velocity-position command. Thus, the model shown in Fig. 2E can construct the ‘missing’ eye-velocity-position command during all types of upward eye movement.

4.2. A feedback loop between the VPFL and motoneurons

The model shown in Fig. 2E adopts a simple algorithm for creating slow motor commands during all kinds of upward eye movement. However, a biological system does not necessarily follow a simple algorithm.

Fig. 2E suggests that the firings of the neurons in the MN are inputted into the group of neurons that creates the slow motor command. In other words, the group of neurons receives an efference copy of firings of the MN. However, no research has identified neural groups that receive fibers from the MN, while collaterals of fibers projecting into the MN were reported to project to the interstitial nucleus of Cajal (INC) (Iwamoto et al., 1990b; Moschovakis et al., 1991a,b). The INC may receive an eye acceleration-velocity-position command like the MN. Anatomically, neural circuits between the cerebellar flocculus and the MN that are assumed to function during vertical OFR have been reported (Fig. 3A) (for a review, see Fukushima et al., 1992). The firing of Purkinje cells of the cerebellar flocculus is transmitted to the VN (Zhang et al., 1995). The axons of the neurons in the VN project to the MN, and their branches project to the INC (Fukushima, 1987; Iwamoto et al., 1990b). Some neurons in the INC project axons to the MN, which is involved in vertical eye movement (Carpenter et al., 1970; Graybiel and Hartweg, 1974; Kokkoroyannis et al., 1996; Steiger and Buttner-Ennever, 1979), and some project axons to the VN (Carpenter and Cowie, 1985; Chimoto et al., 1992; Fukushima et al., 1982; Kokkoroyannis et al., 1996; Pompeiano and Walberg, 1957). The two sides of the VN are interconnected (Brodal, 1974). Thus, the vestibular nuclei-interstitial nucleus of Cajal-vestibular nuclei (VN-INC-VN) circuit might function as a closed-loop circuit, as modeled in Fig. 2E.

The low pass filter in Fig. 2E receives the same input as input into the MN. The reported differences between INC firing and MN firing (for a review, see Fukushima et al., 1992) suggest that the input into the INC might be different from the input into the MN. To construct the ‘missing’ eye velocity-position command using a second order low-pass filter, the input into the low-pass filter must have eye acceleration-velocity-position information, but not necessarily be the same as the final motor

command. This suggests that the model in Fig. 2E can be replaced by that in Fig. 3B. Even if the input into the INC is different from the input into the MN, the input into the INC is assumed to have eye acceleration-velocity-position information because the INC receives input from fibers that convey dynamic and slow motor commands (Iwamoto et al., 1990b). Thus, the low-pass filter in Fig. 3B constructs the ‘missing’ eye velocity-position command from an eye acceleration-velocity-position command that is different from the final motor command.

The circuit in Fig. 3A will produce eye-velocity-position commands not only during upward OFR, but also during upward VOR and upward saccades, because the INC is assumed to receive the collaterals of fibers projecting into the MN conveying information during not only vertical OFR, but also vertical VOR and vertical saccades. During vertical VOR, the head-velocity information of the primary vestibular afferent is sent to the flocculus-target-neuron and position-vestibular-neuron in the VN (Zhang et al., 1995). VN firing is also transported to both the INC and the MN (Iwamoto et al., 1990b). During vertical saccades, the firing information of vertical burst neurons in the rostral interstitial nucleus of the medial longitudinal fasciculus also flows into the INC and the MN (Moschovakis et al., 1991a,b). These preceding studies suggest that the INC receives acceleration-velocity-position commands like motoneurons, not only during vertical OFR, but also during vertical VOR and vertical saccades. If the VN-INC-VN loop corresponds to the circuit in Fig. 3B, the loop would be able to construct the eye-velocity-position command during upward VOR, upward saccades, and upward OFR.

If the VN-INC-VN loop fills the function proposed in Fig. 3B: (1) some neurons in the VN and the INC should have a firing frequency corresponding to the linear sum of eye velocity and position; and (2) lesions of the VN or INC will disrupt neural integration for vertical eye movements. Some physiological data support these predictions: (1) Some neurons in the VN (Iwamoto et al., 1990a) and in and around the INC (Büttner et al., 1977; King and Fuchs, 1977; King et al., 1981; Fukushima, 1987; Fukushima et al., 1990; Shiraishi and Nakao, 1995; Chimoto et al., 1999) exhibit a burst-tonic or tonic firing rate for vertical eye movements; (2) Lesions of the INC or VN shorten the time constant of the neural integrator (Anderson et al., 1979; Cannon and Robinson, 1987; Fukushima, 1987; Crawford et al., 1991). The VN-INC-VN loop has been implicated as an important component of neural integration (Fukushima et al., 1992; Chimoto et al., 1999). Thus, the VN-INC-VN loop might work as shown in Fig. 3B.

Some other structures have been proposed to create the slow motor command, including commissural connections between bilateral INCs (Moschovakis et al.,

1991a,b; Partsalis et al., 1994; Chimoto et al., 1999) and cerebellum (Fukushima et al., 1993; Fukushima and Kaneko, 1995). Chimoto et al. (1999) suggested that multiple loops involving the VN-INC-VN loop, the commissural INC loop, other parts of the brain stem, and possibly the cerebellum might work for neural integration. The low-pass filter in Fig. 3B might be realized as a part of these neural circuits.

4.3. Neural integrator

Robinson (1975) suggested that there must be a neural system, called the neural integrator, which creates eye position from eye velocity during all kinds of conjugate eye movement. Robinson (1975) hypothesized that the neural integrator works commonly during all kinds of conjugate eye movement.

As we described previously, the low-pass filter in Fig. 3B makes the slow motor command from the sum of dynamic and slow motor commands. If the definition of the ‘neural integrator’ is a group of neurons that makes the slow motor command from dynamic motor commands, then the low-pass filter in Fig. 3B is not the ‘neural integrator’. To visualize the difference between the ‘neural integrator’ and our proposed low-pass filter, the diagram in Fig. 3B is redrawn as the diagram in Fig. 3C. The pathway in the yellow box in Fig. 3C corresponds to the ‘neural integrator’, because it makes the slow motor command from dynamic motor commands. In our proposed model, ‘neural integration’ is carried out by a low pass filter in a closed feedback loop.

Some neural network models have been proposed for neural integration (Arnold and Robinson, 1997; Cannon et al., 1983; Galiana and Outerbridge, 1984). All of these models also contain positive feedback closed-loops. However, the purpose of the positive feedback in these models is different from the purpose of the positive feedback in Fig. 3B. Previous neural network models needed positive feedback connections to create slow motor commands, whereas the model in Fig. 2E, Fig. 3B, and Fig. 3C does not need feedback connections to create slow motor commands. The low-pass filters in the figures create slow motor commands, and the feedback connections in the figures are utilized only for the addition of the slow motor command to the dynamic motor command (Fig. 3D).

4.4. Our model's predictions and reliability

Fig. 3D shows how we believe the neural system works for upward OFR control. The dynamic component of a motor command, like the eye acceleration-velocity command, is generated from retinal slip in the feedforward pathway through the VPFL, while a slow motor command, like the eye velocity-position command, comes from a closed internal feedback loop in

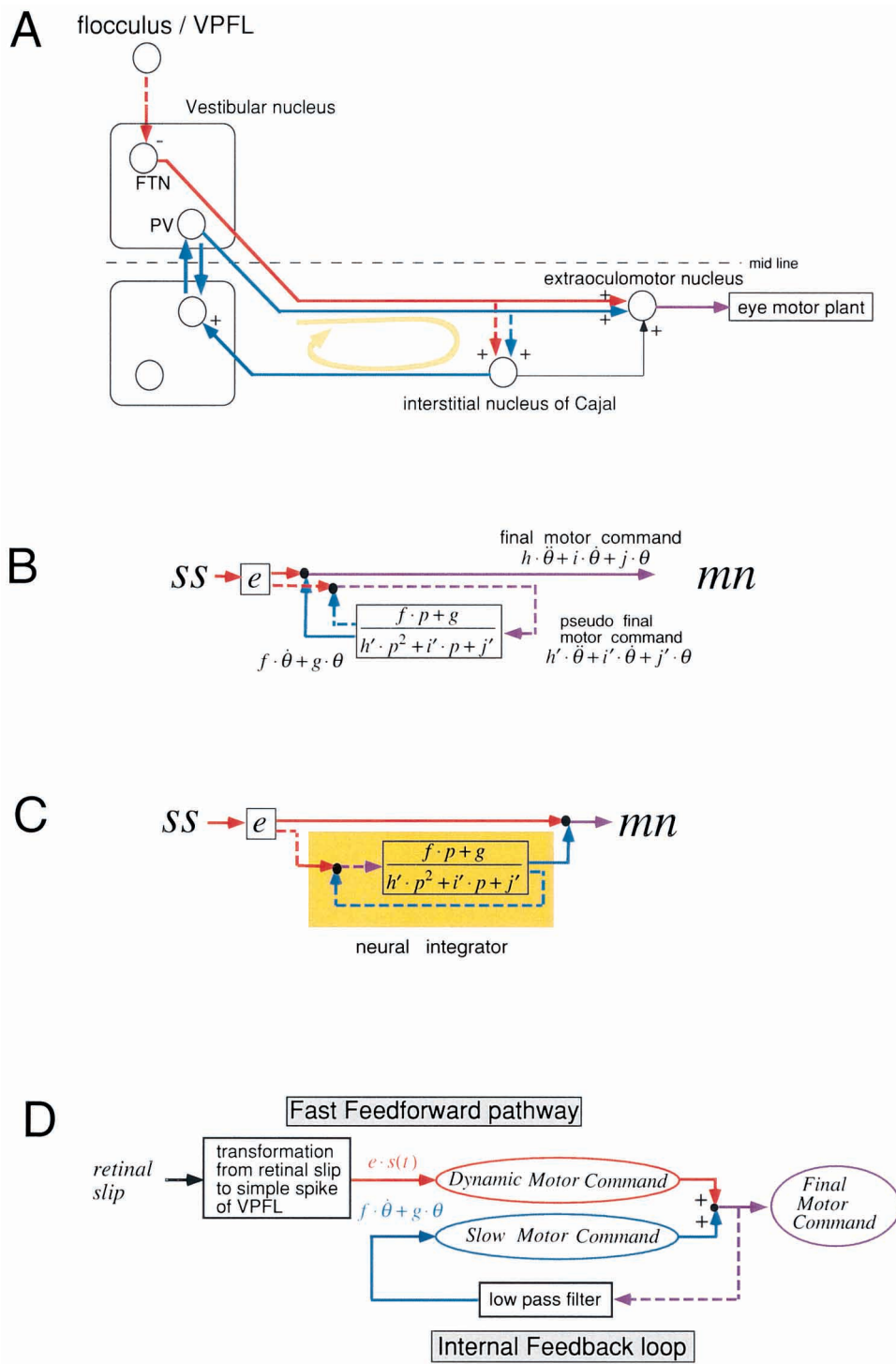


Fig. 3.

the brain stem. It is assumed that the low-pass filter in Fig. 3D contains a kind of forward model (Kawato, 1999) that calculates positional information on eye movement from the final motor command.

If the model in Fig. 3B is realized in the circuit in Fig. 3A, the following predictions can be derived: (1) The firing of some VN neurons has a phase-delay larger

than the MN; (2) Such neurons send axons to the MN and the INC; (3) The temporal pattern of firing of the flocculus-target-neurons in the VN should be successfully reconstructed by the combination of eye acceleration and velocity using inverse dynamics analysis. The temporal firing pattern of the INC should be successfully reconstructed by the combination of eye velocity

and position; (4) The coefficients that are calculated from the inverse dynamics analysis of some VN neurons should not differ for upward OFR, VOR, and saccades.

The data for the 5719 trials in one monkey, we estimated the values of e , f , and g in Fig. 2E to be 0.490, 0.407, and 4.14, respectively. From the data for the 99 trials in the other monkey, the respective estimates were 0.181, 0.389, and 4.14. e denotes the size correction rate between recorded simple spike firing in the monkeys and reported neural firing in the MN by Keller (1973), while f and g denote the characteristics of the system between the VPFL and the MN. The similarity of f and g in the two monkeys supports the existence of our proposed model in the brain stem.

Our model relating the VPFL and eye position (Fig. 1A) corresponds to a second-order low-pass filter model as a transfer function. Krauzlis (2000) proposed a second-order linear model with two poles and one zero for the transfer function between the VPFL/flocculus and eye ‘velocity’ during smooth pursuit. His model successfully constructed eye velocity from simple spike firing frequency, while it could not reconstruct eye velocity well after eliminating the one zero component. However, his results do not mean that the two poles and one zero model is better than our second-order linear low-pass filter model. When a model with one zero component can reconstruct eye velocity well, the model obviously cannot reconstruct eye velocity after eliminating the one zero component without adequate changes in the other time constants. Our model reconstructed upward OFR velocity successfully (the goodness-of-fit was 0.973 for eye velocity and 0.677 for eye acceleration), but it could not reconstruct eye velocity well after adding the one zero component, just as in Krauzlis (2000) (the goodness-of-fit was 0.814 for eye velocity and 0.287 for eye acceleration). If we use the same logic as Krauzlis, these values of goodness-of-fit suggest that our second-order low pass filter model for the system between the VPFL and eye position is better

than the two poles and one zero model for the system between the VPFL and eye velocity. We tried to simulate the temporal pattern of eye velocity using the transfer function used by Krauzlis and our simple spike firing data. The ratio of the size of simple spike firing to the eye movement of the monkeys in Krauzlis (2000) may be different from the ratio in our monkey. We therefore estimated the goodness-of-fit after adjusting the amplitude of the simulated eye movement to our monkey’s eye movement. The goodness-of-fit was 0.958 for eye velocity and 0.195 for eye acceleration. The two poles and one zero model in Krauzlis (2000) could not reconstruct eye acceleration successfully, while our proposed model reconstructed both eye velocity and eye acceleration successfully.

In this paper, we assumed that the final acceleration command comes from simple spikes of the VPFL and the slow motor command is created in the system between the VPFL and the MN. These assumptions are based on the assumption that OFR is controlled by the MST–DLPN–VPFL–MN pathway. Impairment of OFR by flocculus/VPFL lesions (Miles et al., 1986) means that the MST–DLPN–VPFL pathway controls OFR primarily, while the lateral terminal nucleus (LTN) in the accessory optic system (AOS) has been reported to respond to vertical large-field stimulus (Mustari and Fuchs, 1989). Further studies of pathways other than the MST–DLPN–VPFL pathway will be required to determine whether the pathway through the VPFL is the only pathway for OFR control.

Acknowledgements

We are very grateful to Dr H. Gomi for his fruitful discussions with us and thank Drs K. Fukushima and M. Tanaka for their comments on our work, Namba for her secretarial assistance and Drs T. Bando and S. Kitazawa for their encouragement.

Fig. 3. (A) The correspondence between the real neural system for vertical OFR and the circuit shown in Fig. 2E. The red line shows the movement of the dynamic motor command. The blue line shows the movement of the slow motor command. The purple line shows the final motor command. Summation of the dynamic motor command (red line) and slow motor command (blue line) is assumed to construct the final motor command (purple line). The interstitial nucleus of Cajal (INC) receives both dynamic and slow commands. This figure is based on a figure in Fukushima et al. (1992) and a slight modification by the results of Zhang et al. (1995). FTN: flocculus target neuron (Zhang et al., 1995). PV: position vestibular cell. (B) Diagram of the closed-loop circuit for Fig. 3A when the input into the INC is not the same as the final motor command. θ denotes eye movement position. e , f , g , h , i , and j are the same as the values in Fig. 2E. h' , i' , and j' are the coefficients for the eye acceleration, velocity, and position commands for input into the low pass filter, respectively. Although, anatomically the dynamic motor command and slow motor command converge at the extraoculomotor nucleus (mn) as shown in Fig. 3A, the summing junction of the red line and blue line was drawn as a black dot apart from mn to simplify the drawing. (C) Diagram of a closed-loop circuit similar to that in Fig. 3B; the only difference is the input-output direction for the low pass filter. The circuit colored yellow corresponds to the neural integrator, which constructs slow motor commands from dynamic motor commands. (D) Our interpretation of the control system that constructs the final motor command for upward OFR. The final motor command for upward OFR is constructed by summing the dynamic motor command and the slow motor command. The dynamic motor command comes from a fast feedforward pathway, which translates retinal slip information into a motor command. The slow motor command comes from a feedback loop in the brain stem. s denotes the simple spike firing frequency.

References

- Anderson, J.H., Precht, W., Pappas, C., 1979. Changes in the vertical vestibuloocular reflex due to kainic acid lesions of the interstitial nucleus of Cajal. *Neurosci. Lett.* 14, 259–264.
- Arnold, D.B., Robinson, D.A., 1997. The oculomotor integrator: testing of a neural network model. *Exp. Brain Res.* 113, 57–74.
- Becker, W., Klein, H.M., 1973. Accuracy of saccadic eye movements and maintenance of eccentric eye positions in the dark. *Vision Res.* 13, 1021–1034.
- Brodal, A., 1974. Anatomy of the vestibular nuclei and their connections. In: Kornhuber, H.H. (Ed.), *Handbook of Sensory Physiology, Vestibular System*, vol. VI/1. Springer-Verlag, New York, pp. 239–352.
- Büttner, U., Hepp, K., Henn, V., 1977. Neurons in the rostral mesencephalic and paramedian pontine reticular formation generating fast eye movements. In: Baker, R., Berthoz, A. (Eds.), *Control of Gaze by Brain Stem Neurons*. Elsevier, Amsterdam, pp. 309–318.
- Cannon, S.C., Robinson, D.A., Shamma, S., 1983. A proposed neural network for the integrator of the oculomotor systems. *Biol. Cybern.* 49, 127–136.
- Cannon, S.C., Robinson, D.A., 1987. Loss of the neural integrator of the oculomotor system from brain stem lesions in monkey. *J. Neurophysiol.* 57, 93–108.
- Carpenter, M.B., Cowie, R.J., 1985. Connections and oculomotor projections of the superior vestibular nucleus and cell group 'y'. *Brain Res.* 336, 265–287.
- Carpenter, M.B., Harbison, J.W., Peter, P., 1970. Accessory oculomotor nuclei in the monkey: projections and effects of discrete lesions. *J. Comp. Neurol.* 140, 131–154.
- Chimoto, S., Iwamoto, Y., Yoshida, K., 1992. Projection of vertical eye movement related neurons in the interstitial nucleus of Cajal to the vestibular nucleus in the cat. *Neurosci. Res.* 15, 293–298.
- Chimoto, S., Iwamoto, Y., Yoshida, K., 1999. Projection and firing properties of down eye-movement neurons in the interstitial nucleus of Cajal in the cat. *J. Neurophysiol.* 81, 1199–1211.
- Crawford, D., Cadera, W., Vilis, T., 1991. Generation of torsional and vertical eye position signals by the interstitial nucleus of Cajal. *Science* 252, 1551–1553.
- Fukushima, K., 1987. The interstitial nucleus of Cajal and its role in the control of movements of head and eyes. *Prog. Neurobiol.* 29, 107–192.
- Fukushima, K., Buharin, E.V., Fukushima, J., 1993. Responses of floccular Purkinje cells to sinusoidal vertical rotation and effects of muscimol infusion into the flocculus in alert cats. *Neurosci. Res.* 17, 297–305.
- Fukushima, K., Fukushima, J., Harada, C., Ohashi, T., Kase, M., 1990. Neuronal activity related to vertical eye movement in the region of the interstitial nucleus of Cajal in alert cats. *Exp. Brain Res.* 79, 43–64.
- Fukushima, K., Kaneko, C.R.S., Fuchs, A.F., 1992. The neural substrate of integration in the oculomotor system. *Prog. Neurobiol.* 39, 609–639.
- Fukushima, K., Ohno, M., Takahashi, K., Kato, M., 1982. Location and vestibular responses of interstitial and midbrain reticular neurons that project to the vestibular nuclei in the cat. *Exp. Brain Res.* 45, 303–312.
- Galiana, H.L., Outerbridge, J.S., 1984. A bilateral model for central neural pathways in vestibuloocular reflex. *J. Neurophysiol.* 51, 210–241.
- Gellman, R.S., Carl, J.R., Miles, F.A., 1990. Short latency ocular following responses in man. *Visual Neurosci.* 5, 107–122.
- Gomi, H., Shidara, M., Takemura, A., Inoue, Y., Kawano, K., Kawato, M., 1998. Temporal firing patterns of Purkinje cells in the cerebellar ventral paraflocculus during Ocular Following Responses in Monkeys. 1. Simple spike. *J. Neurophysiol.* 80, 818–831.
- Graybiel, A., Hartweg, E.A., 1974. Some afferent connections of the oculomotor complex in the cat: an experimental study with tracer techniques. *Brain Res.* 81, 543–551.
- Iwamoto, Y., Kitama, T., Yoshida, K., 1990a. Vertical eye movement-related secondary vestibular neurons ascending in medial longitudinal fasciculus in the cat. 1. Firing properties and projection pathways. *J. Neurophysiol.* 63, 902–917.
- Iwamoto, Y., Kitama, T., Yoshida, K., 1990b. Vertical eye movement-related secondary vestibular neurons ascending in medial longitudinal fasciculus in the cat. 2. Direct connections with extraocular motoneurons. *J. Neurophysiol.* 63, 918–935.
- Kawano, K., 1999. Ocular tracking: behavior and neurophysiology. *Curr. Opin. Neurobiol.* 9, 467–473.
- Kawano, K., Shidara, M., Yamane, S., 1992. Neural activity in dorsolateral pontine nucleus of an alert monkey during ocular following responses. *J. Neurophysiol.* 67, 680–703.
- Kawano, K., Shidara, M., Watanabe, Y., Yamane, S., 1994. Neural activity in cortical area of MST of an alert monkey during ocular following responses. *J. Neurophysiol.* 71, 2305–2324.
- Kawato, M., 1999. Internal models for motor control and trajectory planning. *Curr. Opin. Neurobiol.* 9, 718–727.
- Keller, E.L., 1973. Accommodative vergence in the alert monkey. Motor unit analysis. *Vision Res.* 13, 1565–1575.
- King, W.M., Fuchs, A.F., 1977. Neuronal activity in the mesencephalon related to vertical eye movement. In: Baker, R., Berthoz, A. (Eds.), *Control of Gaze by Brain Stem Neurons*. Elsevier, Amsterdam, pp. 319–326.
- King, W.M., Fuchs, A.F., Magnin, M., 1981. Vertical eye movement related responses of neurons in the midbrain near the interstitial nucleus of Cajal. *J. Neurophysiol.* 46, 549–562.
- Kobayashi, Y., Kawano, K., Takemura, A., Inoue, Y., Kitama, T., Gomi, H., Kawato, M., 1998. Temporal firing patterns of Purkinje cells in the cerebellar ventral paraflocculus during ocular following responses in monkeys. 2. Complex spikes. *J. Neurophysiol.* 80, 832–848.
- Kokkoroyannis, T., Scudder, C.A., Balaban, C.D., Highstein, S.M., 1996. Anatomy and physiology of the primate interstitial nucleus of Cajal. 1. Efferent projections. *J. Neurophysiol.* 75, 725–739.
- Krauzlis, R.J., 2000. Population coding of movement dynamics by cerebellar Purkinje cells. *Neuroreport* 11, 1045–1050.
- Miles, F.A., Kawano, K., Optican, L.M., 1986. Short-latency ocular following responses of monkey. 1. Dependence on temporospatial properties of visual input. *J. Neurophysiol.* 56, 1321–1354.
- Moschovakis, A.K., Scudder, A., Highstein, S.M., 1991a. Structure of the primate oculomotor burst generator 1. Medium-lead burst neurons with upward on-directions. *J. Neurophysiol.* 65, 203–217.
- Moschovakis, A.K., Scudder, A., Highstein, S.M., 1991b. Structure of the primate oculomotor burst generator 2. Medium-lead burst neurons with downward on-directions. *J. Neurophysiol.* 65, 218–229.
- Mustari, M.J., Fuchs, A.F., 1989. Response properties of single units in the lateral terminal nucleus of the accessory optic system in the behaving primate. *J. Neurophysiol.* 61, 1207–1220.
- Partsalis, A.M., Highstein, S.M., Moschovakis, A.K., 1994. Lesions of the posterior commissure disable the vertical neural integrator of the primate oculomotor system. *J. Neurophysiol.* 71, 2582–2585.
- Pompeiano, O., Walberg, F., 1957. Descending connections to the vestibular nuclei. An experimental study in the cat. *J. Comp. Neurol.* 108, 465–504.
- Robinson, D.A., 1975. Oculomotor control signals. In: Lennerstrand, G., et al. (Eds.), *Basic Mechanisms of Ocular Motility and Their Clinical Implications*. Pergamon Press, Oxford, pp. 337–374.

- Shidara, M., Kawano, K., 1993. Role of Purkinje cells in the ventral paraflocculus in short-latency ocular following responses. *Exp. Brain. Res.* 93, 185–195.
- Shidara, M., Kawano, K., Gomi, H., Kawato, M., 1993. Inverse-dynamics encoding of eye movements of Purkinje cells in the cerebellum. *Nature* 365, 50–52.
- Shiraishi, Y., Nakao, S., 1995. Differential locations in the midbrain of distinct groups of vertical eye movement-related neurons in cat: their projections and direct connections with oculomotor neurons. *Acta Physiol. Scand.* 154, 151–163.
- Steiger, H.J., Buttner-Ennever, J.A., 1979. Oculomotor nucleus afferents in the monkey demonstrated with horseradish peroxidase. *Brain. Res.* 160, 1–15.
- Yamamoto, K., Kobayashi, Y., Takemura, A., Kawano, K., Kawato, M., 1997a. A mathematical model that reproduces vertical ocular following responses from visual stimuli by reproducing the simple spike firing frequency of Purkinje cells in the cerebellum. *Neurosci. Res.* 29, 161–169.
- Yamamoto, K., Kobayashi, Y., Takemura, A., Kawano, K., Kawato, M., 1997b. A simulation system for vertical ocular following responses with the simple spike firing rate of Purkinje cells in the cerebellum. *Soc. Neurosci. Abstr.*
- Zhang, Y., Partsalis, A.M., Highstein, S.M., 1995. Properties of superior vestibular nucleus flocculus target neurons in the squirrel monkey. 1. General properties in comparison with flocculus projecting neurons. *J. Neurophysiol.* 73, 2261–2278.

UNCORRECTED PROOF